ACS APPLIED MATERIALS & INTERFACES

RESEARCH ARTICLE

www.acsami.org

Electrospun Polyurethane Fibers for Absorption of Volatile Organic Compounds from Air

Elke Scholten,† Lev Bromberg, Gregory C. Rutledge, and T. Alan Hatton*

Department of Chemical Engineering, Massachusetts Institute of Technology, 77 Massachusetts Avenue, Cambridge, Massachusetts 02139, United States

ABSTRACT: Electrospun polyurethane fibers for removal of volatile organic compounds (VOC) from air with rapid VOC absorption and desorption have been developed. Polyurethanes based on 4,4-methylenebis(phenylisocyanate) (MDI) and aliphatic isophorone diisocyanate as the hard segments and butanediol and tetramethylene glycol as the soft segments were electrospun from their solutions in N,N-dimethylformamide to form micrometer-sized fibers. Although activated carbon possessed a many-fold higher surface area than the polyurethane fiber meshes, the sorption capacity of the polyurethane fibers was found to be similar to that of activated carbon specifically designed for vapor adsorption. Furthermore, in contrast to VOC sorption on activated carbon, where complete regeneration of the adsorbent was not possible, the polyurethane fibers demonstrated a completely reversible absorption and desorption, with desorption obtained by a simple purging with nitrogen at room temperature. The fibers possessed a high affinity toward toluene and chloroform, but aliphatic hexane lacked the necessary strong attractive interactions with the polyurethane chains and therefore was less strongly absorbed. The selectivity of the polyurethane fibers toward different vapors, along with the ease of regeneration, makes them attractive materials for VOC filtration.

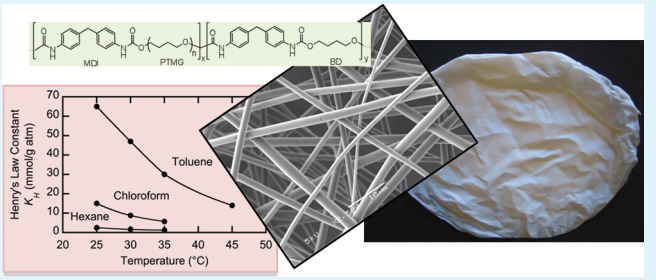

KEYWORDS: regenerable filter, electrospun polyurethane fibers, absorption capacity

1. INTRODUCTION

Significant quantities of volatile organic compounds (VOCs) are emitted into the air, both indoors and outdoors, each year by various sources, including both deliberate and fugitive emissions from industrial plants, vehicles, and aircraft. The presence of indoor VOCs is associated with odors and health effects such as sensory irritation and the more complex set of symptoms known as Sick Building Syndrome (SBS). More recently, a possible link between the increase in allergies and exposure to VOCs has been suggested, and the number of complaints in aircraft of unpleasant odors and cabin environment has increased significantly.[1] VOC removal from a large diversity of sources is thus desirable to decrease the negative health risks in both outdoor and indoor environments.

Among the various methods for VOC abatement,[2] adsorption has been regarded as one of the most effective ways to decrease VOC levels and to improve air quality. Activated carbons have generally been a logical choice for the removal of VOCs from air streams as their high surface area and large pore volume enable their adsorption at low concentrations. However, disadvantages in using activated carbons include high pressure drops over the adsorbent bed, a decrease in adsorption capacity after the initial adsorption (carbon fouling) and the difficulty of regeneration of the activated carbon on site. Conventionally, activated carbons are regenerated[3] by steam desorption of the adsorbed VOC followed by optional drying and cooling steps. The steam-air-solvent vapor mixture is then condensed and sent to appropriate separation devices. Water remaining in the bed can be exhausted to the atmosphere. The two optional steps are required if water is detrimental to the adsorption or if the hot carbon acts as a catalyst for the conversion of the solvent. Because of these difficulties in regeneration of activated carbon, these filter types are often discarded after a single cycle and are not reused.

In many of the applications for removal of trace organic compounds from enclosed environments, it is desirable to be able to regenerate the adsorbents under ambient conditions of temperature and pressure. To circumvent the problems associated with carbon adsorbents, and to enable air filters to be used multiple times, alternative approaches to increase the efficiency of the adsorption process and to enhance the regeneration of the adsorbents have been considered.

The adsorbent materials (carbon) are usually obtained in a powder or granular form, which in many cases may constrain their use. The inclusion of adsorbent materials in other forms might be advantageous; for instance, the incorporation of activated carbon in more flexible matrices to form activated carbon fabric (ACF) cloths allows the pressure drop problems to be circumvented,[4] but regeneration of the adsorbent is still an unresolved issue. The large adsorption capacity of activated carbon can be ascribed to its large internal pore surface area, which suggests that utilization of adsorbents in structures with very small diameters (thus large surface areas) is of interest and is,

Received: June 9, 2011
Accepted: September 3, 2011
Published: September 03, 2011

indeed, becoming more popular.[5,6] One option is to increase the surface area of the adsorbent material by its fabrication in the form of fibrous materials. In this paper, we show that electrospun polyurethane fibers have high sorption capacities and rapid sorption and desorption rates for VOCs.

Polymer solutions have been used extensively for the spinning of variously sized fibers,[7−13] and over the past decade or so, much attention has been paid to the production of core-shell,[14,15] hollow, and porous[16−18] electrospun fibers for applications in the field of applied nanotechnology where they have also been surface-modified to provide specific thermal, chemical and biomedical protection capabilities.[19−21] Electrospun fibers have been investigated widely[22−24] for medical sensors and photonics,[25] tissue engineering scaffolds,[26,27] wound dressing materials,[28] waterproof breathable fabrics,[29] vascular graft,[30] and antimicrobial applications.[31,32] Applications of polyurethane filters based on nanofiber nonwoven meshes prepared by the electrospinning process in air filtration have been implied.[33] It is to be anticipated that these electrospun fibers with their very high surface areas may enable efficient VOC filtration, but to the best of our knowledge, such fibers have not been used for absorption purposes and no comparison of the capacities of activated carbon and electrospun polymeric systems has been made. It is the goal of this work to provide such an assessment.

Polyurethanes have been investigated in the form of foams or membranes for the uptake or separation of organic liquids,[34−39] organic vapors,[40,41] metal ions,[42] and water.[43,44] Pinto and coworkers, in particular, have implemented polyurethane foams as an adsorbent material, reporting that their interactions with various volatile organic compounds enable their use for the adsorption of VOCs to increase the quality of indoor air.[41] Because of the high permeability of water vapor at high temperatures and considerably lower permeability capacity at lower temperatures, these polyurethanes are being coated onto various materials to produce breathable fabrics.[43] Biofilters packed with polyurethane foams inoculated with a mixed microbial population were used successfully to adsorb and degrade toluene.[45] Saeed showed that polyurethane foams also have strong selectivity for specific metal ion adsorption and that this adsorption is an endothermic process.[42]

These polyurethane systems are promising alternatives to activated carbon as adsorbent materials, and should be particularly effective for VOC removal in the form of non-woven fibrous mats. In the present work we have designed polyurethane fibers with VOC removal efficiencies comparable to those of activated carbon, but with significantly easier regeneration through complete desorption of the adsorbed VOC at room temperature on purging with a neutral gas steam. The implementation of nonwoven polyurethane fiber mats might be able to overcome the problems related to the use of the carbon powder.

In this paper, we focus on VOC filters consisting of polyurethane fibers. By varying the ratio between rigid and flexible diol constituents within the polymers, structural properties of the polyurethanes can be altered to vary the structures of polyurethane fiber mats from rubberlike to crystalline.[22,38,44,46−49]

2. EXPERIMENTAL SECTION

Chemicals. 4,4-Methylenebis(phenyl isocyanate) (MDI, 98%), butanediol (BD), isophorone diisocyanate (IPDI, 98%), and poly(tetramethylene glycol) (PTMG, M_W 2000) were all purchased from Sigma-Aldrich Chemical Co. and used as received. Organic solvents N,

Scheme 1. Structure of the MDI-Based Polyurethane

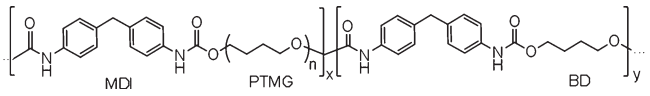

Scheme 2. Structure of the Isophorone-Based Polyurethane

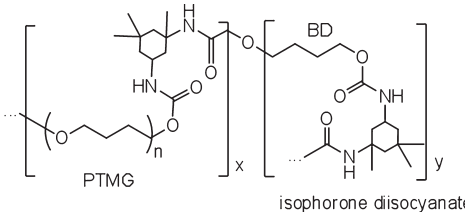

N-dimetylformamide (DMF), tetrahydrofuran (THF), acetone, hexane, chloroform and toluene were purchased from commercial sources and were of highest purity available. The solvents were dried using molecular sieves (3 Å) prior to use. Granular activated carbon (GC 4-10B, nominal surface area, 1000 m^2/g, derived from bituminous coal) was obtained from General Carbon Corporation (Paterson, NJ). This activated carbon was designed for vapor phase applications including the adsorption of organic contaminants from vapor streams.

Polymer Synthesis. The MDI-based polyurethane was synthesized by polycondensation as follows. MDI solution (17.3 g, 69.2 mmol) in 200 mL of anhydrous THF was mixed with PTMG (27.7 g, 13.8 mmol) and 0.1 mL of dibutylin dilaurate under anhydrous conditions. The resulting mixture was kept at 70 °C with reflux for 16 h, and then 5.0 g (55.4 mmol) of BD were added. The above ratio between soft and hard segments was chosen based on its reported spinnability.[46] The resulting solution was kept at 70 °C for 3 h, at which point the viscosity of the solution did not change further, indicating that the reaction had been completed. The viscous solution was allowed to equilibrate at room temperature and the remaining solvent was evaporated in air. The polymer (Scheme 1), with a hard segment content of 45% by weight, was dried at 70 °C until constant weight. In the FTIR spectrum of the polymer, the isocyanate signal at 2270 cm^{-1} disappeared and a band at 1730 cm^{-1} appeared instead, which is indicative of the >C═O stretch in formed urethane groups. A model polyurethane-urea derivative of MDI was synthesized by polymerizing a 10 wt % MDI solution in toluene with added 1.5 wt % triethanolamine and 1.5 wt % water at 70°C for 3 days followed by removal of all solvents under vacuum until constant weight.

The IPDI-based polyurethane was synthesized from a solution of isophorone diisocyanate (IPDI, 8.9 g, 40.0 mmol) and PTMG (4 g, 2 mmol) and 0.1 mL of dibutylin dilaurate in 100 mL of dried THF that was kept at 70 °C for 16 h. The resulting prepolymer was capped with 3.4 g (38 mmol) of BD, following which the solvent was evaporated at 80 °C. The molar ratio of the long PTMG to the short BD was 1:19 and the IPDI-based polyurethane (Scheme 2) possessed a hard segment content of 75 wt %. FTIR spectra of the polyurethane showed that the isocyanate signal at 2270 cm^{-1} was absent and was replaced by the urethane band at 1730 cm^{-1}.

Electrospinning. The MDI-based polyurethane was dissolved in DMF at 32 wt %. The resulting viscous solution was loaded into a 10 mL syringe that was connected to a spinneret. The polymer solution was fed through the spinneret at a speed of 0.02 mL/min and a voltage of 10 kV. A stable jet was formed and the resulting fibers were collected on aluminum foil at a distance from the spinneret of approximately 20 cm. The IPDI-based polyurethane was dissolved in DMF at concentrations in the range of 40−60 wt %. The solutions were fed through the

spinneret at a speed of 0.01 mL/min and the voltage was set at 30 kV. The fibers were collected at a distance of approximately 20 cm. The fiber mats were removed from the foil and were dried in a vacuum oven at 3.7 kPa to prevent the fibers from welding together by traces of solvent not yet removed during the electrospinning process. The fibers were further dried at 1×10^{-3} Pa vacuum.

Thermal Analysis. Glass transition and melting temperatures of the polyurethane fiber mats were obtained using differential scanning calorimetry (DSC Model Q1000, TA Instruments, Inc.). After equilibrating at −90 °C for 3 min, the fiber mats loaded into aluminum pans were heated to 180 °C at 10 °C/min and the heating thermograms were recorded.

Fiber Morphology. The morphology of the electrospun polyurethane fibers was visualized using a JEOL JEM-9310 scanning electron microscope (SEM). Small parts of the non-woven fiber mats were transferred onto a SEM sample holder and were sputtered with gold or palladium for 20−30 s. Surface area of the polyurethane fiber was measured using an ASAP 2010 apparatus (Micromeritics Instrument Corp., Norcross, GA). The polyurethane non-woven fiber mat was cut into small pieces of 5 × 5 mm in order to fill the sample holder of the apparatus. The sample was first degassed by heating to approximately 100 °C at low pressure, and then transferred into a liquid nitrogen bath and cooled down to −196 °C. The adsorption and desorption curves were constructed via changing the relative pressure inside the sample holder and recording the change of adsorbed nitrogen on the polyurethane fibers.

Adsorption Experiments. For the adsorption experiments with both polyurethane fiber mats and activated carbon, we used a magnetic suspension balance (Rubotherm, Bochum, Germany) fed through stainless steel tubing with a stream of nitrogen at a flow rate of 100 mL/min (1.25 mg/min) regulated with a flow controller (Aalborg, Orangeburg, NY). The nitrogen stream was first passed through a temperature-controlled chamber, where the gas was allowed to reach its desired temperature (25−45 °C), and then entered the sample chamber, where a small sample holder was filled with the non-woven fiber mat or activated carbon. After the weight of the fibers in the sample stabilized, a pump was turned on allowing the selected solvent to be injected into a heating chamber, where it vaporized and was mixed with the flowing nitrogen stream. The VOC concentration in the nitrogen stream was controlled by varying this pumping rate. The adsorbent was challenged with the nitrogen/vapor mixture of known composition, during which its weight increased and then plateaued, indicating that equilibrium had been reached. The fiber absorption capacity was calculated as $C = [(M/M_0) - 1]$ g/g fiber, where M and M_0 are the equilibrium and initial masses of the sample, respectively. Both the fibers and the activated carbon were dried at 1×10^{-3} Pa and were transported in a closed system while performing the absorption/desorption experiments.

3. RESULTS AND DISCUSSION

The electrospun polyurethane fibers had smooth, non-porous surfaces and an average diameter of approximately 2 μm, as shown for MDI- and isophorene-based fibers in SEM photographs a and b in Figure 1. The uniformity of the MDI-based polyurethane fiber diameters and mat density is also clear from Figure 1c, while the strength and elasticity of these mats are evident from the lack of tearing or breaking of stretched mats held in place with push pins.

A BET analysis of the measured nitrogen adsorption isotherms given in Figure 2 for the MDI-based polyurethane fibers yielded a total surface area of ca. 1.3 m^2/g, a value consistent with that estimated by considering the surface area per unit volume of 2 μm diameter cylindrical fibers. Such a surface area is 770-fold smaller than the manufacturer-quoted 1000 m^2/g- nominal

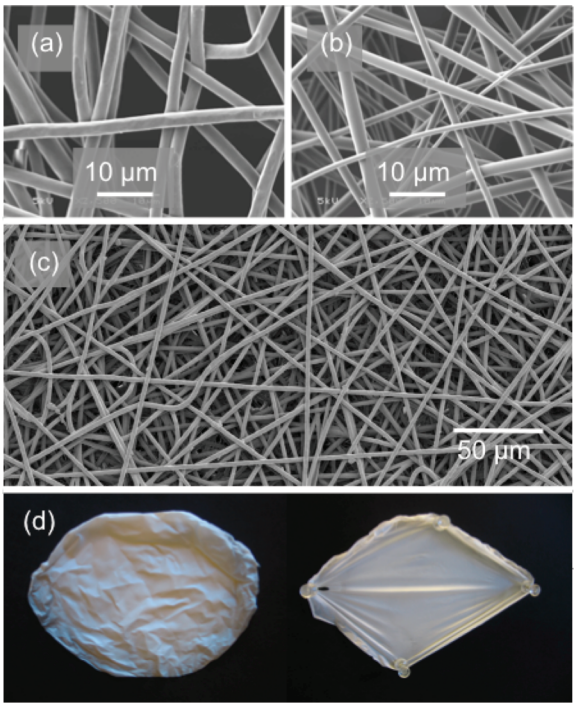

Figure 1. SEM images of (a) MDI-based and (b) isophorone-based nonwoven fiber mats showing smooth, non-porous fiber surfaces. (c) SEM image showing uniformity of MDI-based PU fiber diameter and mat density. (d) Strength and elasticity of mats demonstrated by lack of tearing or breaking of stretched fiber mat held in place with push pins.

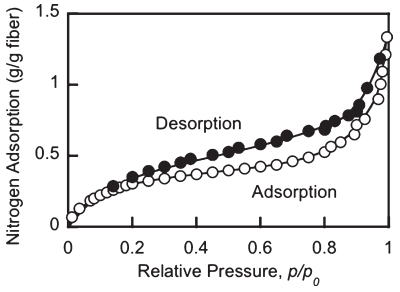

Figure 2. BET Isotherms for liquid nitrogen on nonwoven MDI-based polyurethane fibers.

surface area of typical activated carbons designed specifically for gas adsorption. The hysteresis loop between the adsorption and desorption isotherms is characteristic of a type IV isotherm according to the IUPAC classification[50,51] and indicated the presence of capillary condensation. As both the SEM images and the BET results indicated that the polyurethane fibers were nonporous, we attribute this effect to capillary condensation in the high curvature regions at the intersections of the fibers. We were not able to measure the adsorption of nitrogen onto the IPDI-based polyurethane fibers, which were too fragile to be loaded into the sample holder without damage. Based on the SEM images (Figure 1), we assumed that the IPDI-based polyurethanefibers were nonporous as well.

Figure 3a shows a typical DSC thermogram of the MDI-based polyurethane fiber, which exhibited a soft-segment glass transition at 3°C, and melting peaks at 73 and 135°C characterized by 5.8 and 2.3 J/g melting enthalpies, respectively. Analogous

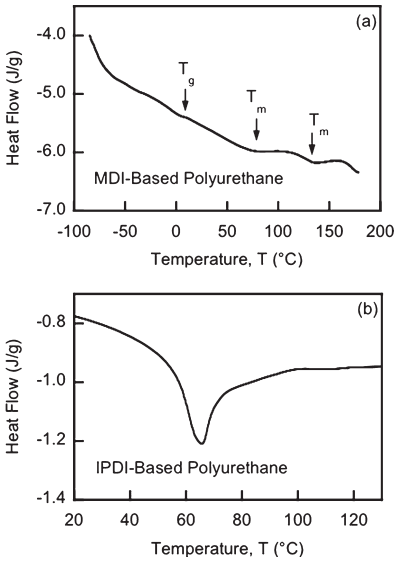

Figure 3. DSC heating thermograms observed with (a) MDI- and (b) isophorone-based polyurethane fiber mats.

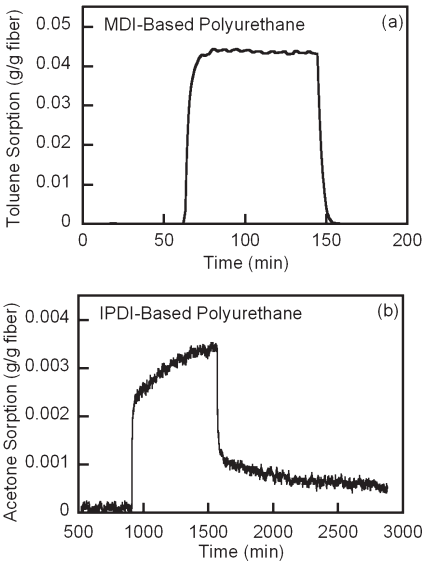

Figure 4. Sorption and desorption behavior for (a) toluene in rubbery MDI-based polyurethane fibers and (b) acetone in crystalline isophorone-based polyurethane fibers. The gas phase concentrations were 2% of their saturation values.

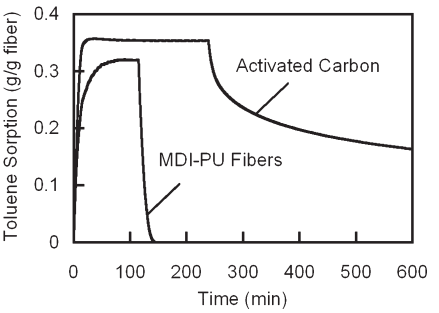

Figure 5. Differing sorption and desorption behavior of toluene with activated carbon and MDI-based PU fibers at 25 °C.

transitions in MDI-based polyurethane have been reported previously.[52−54] The transition at 73°C is related to disordering of single MDI sequences, while the transition at 135°C is attributed to breakage of a long-range order within non-crystalline domains.[52] The thermogram of the polyurethane-urea derivative of MDI, the structure of which could be regarded as 100% crystalline, showed melting peaks at 76°C (12.4 J/g) and 160°C (9.9 J/g). Comparison of the melting enthalpies of the peaks of the two samples provides information on the degree of crystallinity of the MDI-based polyurethane: % crystallinity = $100 \times \Delta H_{PU}/\Delta H_{PU-Urea}$. The melting peak indicated a crystallinity of 47%, in agreement with the MDI content of 45 wt % set in the polyurethane synthesis (see Experimental Section). Given the low glass transition temperature (3 °C), our polyurethane fibers were rubbery within the temperature range of 25−45°C, as also evident from the photograph in Figure 1a.

A heating cycle for the IPDI-based polyurethane fiber mats (Figure 3b) gave a single melting peak T_m at 65 °C, with a melting enthalpy of 6.5 J/g, indicating that this polyurethane was crystalline. The hard segment content was 75 wt %, calculated from the ratio between the hard isocyanate segments and the soft diol segments. The IPDI-based polyurethane fibers were fragile and unable to withstand stretching. Previous studies[54] demonstrated that IPDI-based polyurethane possesses an elastoplastic rather than rubberlike behavior at hard segment contents larger than 60%, in accordance with our results.

Absorption Characteristics of Polyurethane Fibers. Figure 4 depicts sorption and desorption behavior for the MDI-based and IPDI-based polyurethane fibers. Toluene was used to challenge the MDI-based fibers (Figure 4a), whereas acetone was used for the IPDI-based fibers (Figure 4b); these VOCs were selected based on their chemical similarities to the polymer building blocks, and were used at a concentration of 2 percent in the gas phase. As is seen from the shape of the sorption curves in Figure 4a, the polyurethane fibers attained their maximum absorption capacity within approximately 30 min and the process was totally reversible; all sorbed VOC was removed on purging with nitrogen. The large capacity of the fibers for toluene suggested that the toluene was absorbed within the fibers, and was not simply adsorbed on the fiber surfaces. These results are different from the adsorption/desorption history for the crystalline fibers when exposed to acetone vapors, followed by a nitrogen purge, as shown in Figure 4b. The initial adsorption rate was rather fast but then leveled off to a much slower rate, and even after several hours equilibrium had not been reached. The mass of acetone adsorbed in the early stages was approximately equivalent to that of an acetone monolayer on the outer surfaces of the fibers, assuming a VOC molecular diameter of 7.5 Å, and a fiber density of 1 g/cm^3. The significantly slower subsequent adsorption rate was due to the diffusional resistances within the crystalline fibers themselves. Because of the superior absorption behavior of the rubbery MDI-based polyurethane fibers (Figure 4a), all further experiments concentrated on the absorption characteristics of these fibers.

Comparison between VOC Uptake by Polyurethane Fibers and Activated Carbon. Figure 5 shows that the sorption capacities of the activated carbon and the MDI-based polyurethane fibers are comparable when exposed to high levels of toluene vapors. For toluene concentrations in the nitrogen stream of 10%, the toluene sorption capacities of activated carbon and MDI-based polyurethane fibers were 35 and 32 wt %, respectively,

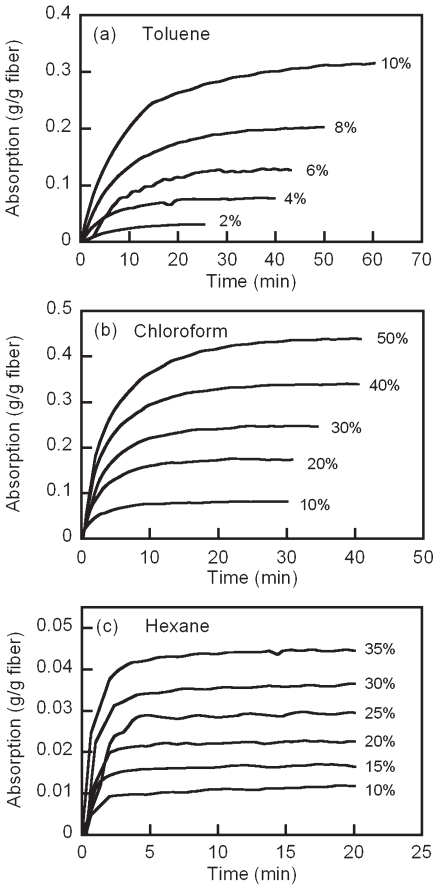

Figure 6. Absorption of (a) toluene, (b) chloroform, and (c) hexane on MDI-based polyurethane fiber mats at varying VOC concentrations (wt %).

similar to the adsorption capacities found previously for toluene on activated carbons.[55] The high adsorption capacity of activated carbon for VOCs is the result of interactions of the solutes with a number of different functional sites present in high concentration on the large surface area provided by the high pore density.[56] Although the total surface area of the polyurethane fibers (1.3 m^2/g) is over 770-fold smaller than that of the activated carbon because of the lack of pores, the sorption capacity is comparable to that of activated carbon. This underscores the different mechanisms of specific sorption of toluene by the carbon and the polyurethane fibers. The large difference in the total surface areas indicates that the VOC compounds were not only adsorbed onto the surfaces of the polyurethane fibers (as in the case of activated carbon) but were also absorbed within the polymer matrices themselves.

The different mechanisms of sorption in carbon particles and polyurethane fiber mats are also reflected in the differences in their regeneration rates. As is seen in Figure 5, only about 40% of the solvent initially adsorbed by activated carbon desorbed after 5 h of purging by nitrogen, in clear contrast to the behavior observed with the polyurethane fibers, from which 100% of the absorbed toluene desorbed within 20 min of purging. Using 7.5 Å for the molecular size of toluene, we calculated that the maximum monolayer absorption of toluene onto carbon would be approximately 27 wt %. Loadings exceeding this value indicate multilayer adsorption and/or capillary condensation. In the desorption process, the physisorbed multilayers will be desorbed first,

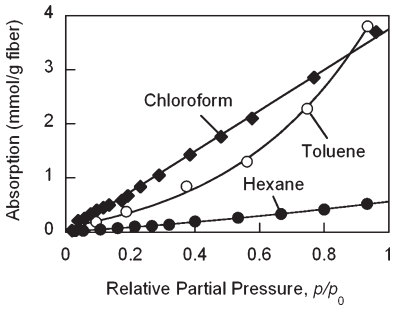

Figure 7. Absorption capacity of MDI-based polyurethane fibers for toluene, chloroform and hexane as affected by the VOC partial pressure at 25 °C.

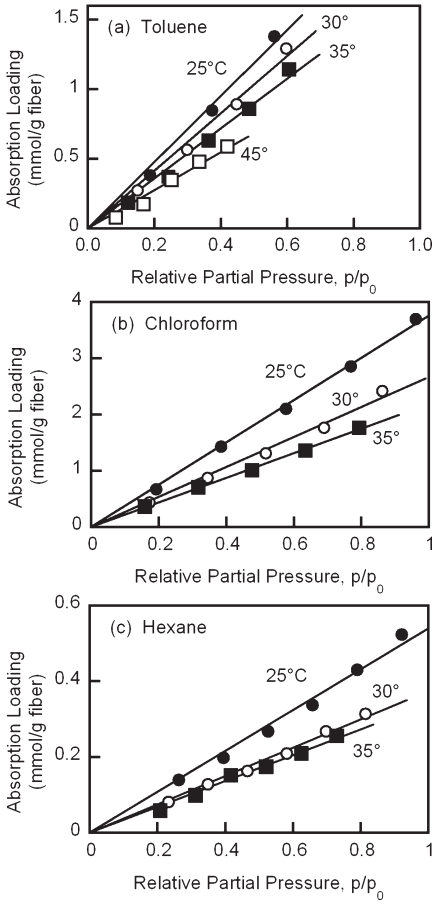

Figure 8. Sorption isotherms for toluene, chloroform, and hexane on MDI-based polyurethane fibers at different temperatures.

while the remaining chemisorbed monolayer of toluene is strongly bound to the carbon pore surfaces.

In the absence of heating, the total adsorbed VOC did not desorb from the activated carbon, and even after 40 h (not shown), a large fraction of the VOC was still present on the carbon adsorbent. When the activated carbon was reused in a second cycle at a vapor phase concentration of 10%, the maximum adsorbed amount of toluene was again 35%, but because the baseline was now at 10%, this represented a decrease in working capacity to 25 wt % compared to the 35 wt % achieved in the first cycle with fresh activated carbon (not shown).

Table 1. Henry's Law Constants for Toluene, Chloroform, and Hexane

	Henry's law constant, K_H (mmol/g_{fiber} kPA)			
VOC	25 °C	30 °C	35 °C	45 °C
toluene	0.642 ± 0.059	0.464 ± 0.020	0.296 ±0.008	
chloroform	0.148 ± 0.002	0.087 ± 0.002	0.0563 ± 0.0005	0.0138 ± 0.0059
hexane	0.0247 ± 0.0004	0.0158 ± 0.0003	0.0118 ± 0.0003	

For effective sorbents, facile desorption processes are important for solvent recovery and recycling or disposal, as well as for adsorbent regeneration and reuse. The inability to regenerate the activated carbon under mild, ambient conditions argues against their use as adsorbents, and purging with a neutral gas is more economical than methods such as steam or vacuum stripping and/or electrothermal treatment that are necessary to regenerate the carbonaceous adsorbents.[55−58] The ease of regeneration of the polyurethane non-woven fibers combined with a capacity comparable to that of activated carbon, suggests that they would be an attractive alternative to conventional VOC sorbents.

Fiber Selectivity for Organic Vapors. The interaction of the polyurethane building blocks with the VOC compounds determines their absorption capacity and selectivity towards different VOCs. The selectivity of the fibers was demonstrated by challenging the fibrous mats with toluene, chloroform and hexane at different vapor partial pressures and temperatures. Figure 6 presents the absorption of the different VOC vapors into the polyurethane fibers at varying concentrations of VOC in nitrogen at a temperature of 25 °C. Regardless of the VOC nature, the absorption of its vapor occurred within the time span of an hour. The equilibrium uptake capacities for these compounds are similar to those obtained when polyurethane foams and membranes were challenged with organic liquid mixtures[34,36,38,39] or vapors.[40,41] Our uptake rates were significantly better than those reported in the literature, when available.

Comparison of the capacity of the fibers for different vapors was facilitated by reporting the absorption, C, in terms of mmol/g_{fiber} as a function of the fractional approach to saturation in the vapor phase, expressed as partial pressure, p, relative to the saturated vapor pressure, p_0, at the temperature of interest. The results at 25 °C shown in Figure 7 for the three compounds studied are comparable to the absorption curves for several VOCs in polyurethane foams reported by Pinto and coworkers.[41]

Although the absorption plots for chloroform and hexane were linear, i.e., these systems exhibited ideal behavior over the whole concentration range, the absorption of toluene was strongly non-ideal at higher concentrations. The relation between the absorption and partial pressure in the linear regime can be described by Henry's law, given by[59,60]

$$C = K_H p \quad (1)$$

where C is the capacity of the fibers at partial gas pressure of p, and K_H is Henry's Law constant. Henry's law is a good representation of the behavior of gases dissolved in liquids or solids at reasonably low concentrations. At higher concentrations, deviations from Henry's law are more pronounced, as can be seen for the absorption of toluene (Figure 7).

Absorption curves were recorded at temperatures between the glass transition temperature and the temperature of the first melting peak of the MDI-based polyurethane shown in Figure 4a,

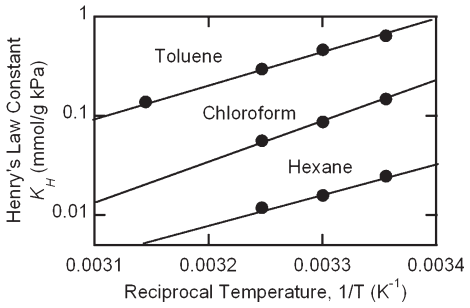

Figure 9. Van't Hoff plots of the Henry's Law constant variations with reciprocal temperature for toluene, chloroform, and hexane.

over a range of 25−45°C .The temperature dependency of the absorption capacity for the three compounds of interest is shown in Figure 8. The K_H values, listed in Table 1, were calculated from the slopes of these lines divided by the corresponding saturated vapor pressures, and therefore reflect the effect of temperature on both these quantities. Note that for toluene the constant was determined using the linear regime only. The Henry's Law constants were largest for toluene, intermediate for chloroform and smallest for hexane. Thus, the fibers possessed a high affinity for toluene and chloroform and a low affinity for hexane. This can be explained by the polar nature of the aromatic and chlorinated VOC compounds and their ability to interact with the building blocks of the polyurethane. Chloroform is a polar solvent with characteristic dipole−dipole interactions with the polyurethane chains; the sorption capacity of such polymers is known also to increase with increasing size of chlorinated solvents.[61] The dispersion van der Waals forces as well as dipole and $\pi-\pi$ interactions between toluene and the polyurethane result in the strong deviation from Henry's law observed at the higher vapor concentrations.[34,36,39] Pinto et al.[41] demonstrated similar adsorption behavior and selectivity in their polyurethane foams, but the sorption rates were not reported. The results of their thermodynamic analysis based on suitable activity coefficient models to allow for these deviations from ideality would also be applicable to this work.

The van't Hoff expression

$$\ln K_H = \frac{-\Delta H}{RT} + \frac{\Delta S}{R} \quad (3)$$

shows that the Henry's Law constant should vary inversely with temperature, depending on the enthalpy, ΔH. This latter thermodynamic quantity was estimated for each of the compounds tested from the slope of the corresponding plot of ln K_H versus reciprocal temperature, $1/T$, shown in Figure 9. The negative ΔH values of −61 ± 2.4, −74 ± 3.7, and −56 ± 6.5 kJ/mol for toluene, chloroform, and hexane, respectively, indicate that the sorption process was exothermic and that strong attractive forces

were present between the fibers and the vapors.[62] These results are in contrast to the endothermic processes with $\Delta H \approx 50$ kJ/mol reported for polyurethane samples immersed in various solvents,[34] in which this endothermicity was attributed to the creation of new pores within the polymers, a different uptake process than operative in our sorption studies.

4. CONCLUSION

We have demonstrated that suitably selected polyurethanes can be electrospun to prepare fiber mats with high sorption capacities for volatile organic solvents. These fibrous mats can be regenerated readily by desorption under ambient conditions, which contrasts favorably with the harsh thermal treatments for regeneration needed to remove the chemisorbed monolayer on the exposed surfaces of activated carbon adsorbents. Thus, fibrous adsorbent mats could find ready use in applications that require benign operating conditions and repeated cycling of the sorbents with easy on-site regeneration without extensive heating and washing processes. The MDI-based polyurethane fiber mats used in this work are robust and elastic, which points to their being able to be formed and used in many process configurations, such as packed beds, spiral-wound membrane systems, etc. Such polyurethane fibers can, in principle, be designed to adsorb specific VOCs depending on the building blocks used in their synthesis.

AUTHOR INFORMATION

Corresponding Author

*E-mail: tahatton@mit.edu. Phone: 617 253 4588. Fax: 617 253 8723.

Present Addresses

[†]Food Physics Group, Department of Agrotechnology and Food Sciences, Wageningen University, Bomenweg 2, 6703 HD Wageningen, The Netherlands

ACKNOWLEDGMENT

This work was supported in part by the Boeing Corporation. E.S. thanks NWO (Netherlands organization of Scientific Research) for support through a Talent Scholarship.

REFERENCES

(1) Lindgren, T.; Norback, D. *Indoor Air* **2002**, *12*, 263–272.
(2) Majumbar, S.; Bhaumik, D.; Sirkar, K. K.; Simes, G. *Environ. Prog.* **2001**, *20*, 27–35.
(3) Wankat, P. C.; Partin, L. R. *Ind. Eng. Chem. Process Des. Dev.* **1980**, *79*, 446–451.
(4) Singh, K. P.; Mohan, D.; Tandon, G. S.; Gupta, G. S. D. *Ind. Eng. Chem. Res.* **2002**, *41*, 2480–2486.
(5) Montefusco, F. *Filtr. Sep.* **2005**, *42*, 30–31.
(6) Duran, A. *Filtr. Sep.* **2004**, *41*, 24–26.
(7) Rutledge, G. C.; Fridrikh, S. V. *Adv. Drug Delivery Rev.* **2007**, *59*, 1384–1391.
(8) Frenot, A.; Chronakis, I. S. *Curr. Opin. Colloid Interface Sci.* **2003**, *8*, 64–75.
(9) Chronakis, I. S. *J. Mater. Process Technol.* **2005**, *167*, 281–293.
(10) Schiffmann, J. D.; Schauer, C. *Polym. Rev.* **2008**, *48*, 317–352.
(11) Dzenis, Y. *Science* **2004**, *304*, 1917–1919.
(12) Subbiah, T.; Bhat, G. S.; Tock, R. W.; Parameswaran, S.; Ramkumar, S. S. *J. Appl. Polym. Sci.* **2005**, *96*, 557–569.
(13) Huang, Z. -M.; Zhang, Y. -Z.; Kotaki, M.; Ramakrishna, S. *Compos. Sci. Technol.* **2003**, *63*, 2223–2253.
(14) Yu, J. H.; Fridrikh, S.; Rutledge, G. *Adv. Mater.* **2004**, *16*, 1562–1566.
(15) McCann, J. T.; Li, D.; Xia, Y. *J. Mater. Chem.* **2005**, *15*, 735–738.
(16) Bognitzki, M.; Czado, W.; Frese, T.; Schaper, A.; Hellwig, M.; Steinhart, M.; Greiner, A.; Wendorff, J. *Adv Mater.* **2001**, *13*, 70–72.
(17) Li, D.; Xia, Y. *Adv. Mater* **2004**, *16*, 1151–1170.
(18) Yang, Y.; Centrone, A.; Chen, L.; Simeon, F.; Hatton, T. A.; Rutledge, G. C. *Carbon* **2011**, *49*, 3395–3403.
(19) Chen, L.; Bromberg, L.; Schreuder-Gibson, H.; Walker, J.; Hatton, T. A.; Rutledge, G. C. *J. Mater. Chem.* **2009**, *19*, 2432–2438.
(20) Chen, L.; Bromberg, L.; Lee, J. A.; Zhang, H.; Schreuder-Gibson, H.; Gibson, P.; Walker, J.; Hammond, P. T.; Hatton, T. A.; Rutledge, G. C. *Chem. Mater.* **2010**, *22*, 1429–1436.
(21) Wang, M.; Hsieh, A. J.; Rutledge, G. C. *Polymer* **2005**, *46*, 3407–3418.
(22) Demir, M. M.; Yilgor, I.; Yilgor, E.; Erman, B. *Polymer* **2002**, *43*, 3303–3309.
(23) Zhuo, H.; Hu, J.; Chen, S.; Yeung, L. *J. Appl. Polym. Sci.* **2008**, *109*, 406–411.
(24) Buruaga, L.; Sardon, H.; Irusta, L.; Gonzalez, A.; Fernandez-Berridi, M. J.; Iruin, J. J. *J. Appl. Polym. Sci.* **2009**, *115*, 1176–1179.
(25) Dersch, R.; Steinhart, M.; Boudriot, U.; Greiner, A.; Wendorff, J. H. *Polym. Adv. Technol.* **2005**, *16*, 276–282.
(26) Pham, Q. P.; Sharma, U. M.; Mikos, A. G. *Tissue Eng.g* **2006**, *12*, 1197–1211.
(27) Caracciolo, P. C.; Buffa, F.; Thomas, V.; Vohra, Y. K.; Abraham, G. A. *J. Appl. Polym. Sci.* **2011**, *121*, 3292–3299.
(28) Yan, L.; Si, S.; Chen, Y.; Yuan, T.; Fan, H.; Yao, Y.; Zhang, Q. *Fibers Polym.* **2011**, *12*, 207–213.
(29) Yoon, B.; Lee, S. *Fibers Polym.* **2011**, *12*, 57–64.
(30) Theron, J. P.; Knoetze, J. H.; Sanderson, R. D.; Hunter, R.; Mequanint, K.; Franz, T.; Zilla, P.; Bezuidenhout, D. *Acta Biomater.* **2010**, *6*, 2434–2447.
(31) Sheikh, F.; Barakat, N. A. M.; Kanjwal, M; Chaudhari, A. A.; Jung, I. −H.; Lee, J. H.; Kim, H. Y. *Macromol. Res.* **2009**, *17*, 688–696.
(32) Yao, C.; Li, X.; Neoh, K. G.; Shi, Z.; Kang, E. T. *J. Membr. Sci.* **2008**, *320*, 259–267.
(33) Sambaer, W.; Zatloukal, W.; Kimmer, D. *Chem. Eng. Sci.* **2011**, *66*, 613–623.
(34) Kendaganna Swamy, B. K.; Siddaramaiah *J. Hazardous Mater.* **2003**, *B99*, 177–190.
(35) Cunha, V. S.; Paredes, M. L.; Borges, C. P.; Habert, A. C.; Norbrega, R. *J. Membr. Sci.* **2002**, *206*, 277–290.
(36) Cunha, V. S.; Nobrega, R.; Habert, A. C. *Braz. J. Chem. Eng.* **1999**, *16*, 297–308.
(37) Singh, R. S.; Rai, B. N.; Upadhyay, S. N. *Process Saf. Environ. Prot.* **2010**, *88*, 366–371.
(38) Kumar, H.; Siddaramaiah *Polymer* **2005**, *46*, 7140–7155.
(39) Lue, J. S.; Peng, S. H. *J. Membr. Sci.* **2003**, *222*, 203–217.
(40) Kamprad, I.; Goss, K.-U. *Anal. Chem.* **2007**, *79*, 4222–4227.
(41) Pinto, M. L.; Pires, J.; Carvallo, A. P.; de Carvalho, M. B.; Bordado, J. C. *J. Phys. Chem. B* **2004**, *108*, 13813–13820.
(42) Saeed, M. M. *J. Radioanal. Nucl. Chem.* **2003**, *256*, 73–80.
(43) Cho, J. W.; Jung, Y. C.; Chun, B. C.; Chung, Y.-C. *J. Appl. Polym. Sci.* **2004**, *92*, 2812–2816.
(44) Ding, X. M.; Hu, J. L.; Tao, X. M.; Wang, Z. F.; Wang, B. *J. Polym. Sci. B: Polym. Phys.* **2005**, *43*, 1865–1872.
(45) Hayashi, J.; Yamamoto, N.; Horikawa, T.; Muroyama, K.; Gomes, V.G. *J. Hazard. Mater.* **2009**, *167*, 275–281.
(46) Cha, D. I.; Kim, H. Y.; Lee, K. H.; Jung, Y. C.; Cho, J. W.; Chun, B. C. *J. Appl. Polym. Sci.* **2005**, *96*, 460–465.
(47) Lai, Y.-C.; Quinn, E. T.; Valint, P. L. *J. Polym. Sci.* **1995**, *33*, 1767–1722.
(48) Laity, P. R.; Taylor, J. E.; Wong, S. S.; Khunkanchoo, P.; Cable, M.; Andrews, G. T.; Johnson, A. F.; Cameron, R. E. *J. Appl. Polym. Sci.* **2006**, *100*, 779–790.

(49) Lee, B. S.; Chun, B. C.; Chung, Y.-C.; Sul, K. I.; Cho, J. W. *Macromolecules* **2001**, *34*, 6431–6437.
(50) Barton, T.; Bull, L. M.; Klemperer, W. G.; Loy, D. A.; McEnaney, B.; Misono, M., 49; Monson, P. A.; Pez, G.; Scherer, G. W.; Vartuli, J. C.; Yaghi, O. M. *Chem. Mater.* **1999**, *11*, 2633–2656.
(51) Balbuena, P. B.; Gubbins, K. E. *Langmuir* **1993**, *9*, 1801–1814.
(52) Finnigan, B.; Halley, P.; Jack, K.; McDowell, A.; Truss, R.; Casey, P.; Knott, R.; Martin, D. *J. Appl. Polym. Sci.* **2006**, *102*, 128–139.
(53) Yang, J. H.; Chun, B. C.; Chung, Y.-C.; Cho, J. H. *Polymer* **2003**, *44*, 3251–3258.
(54) Kim, H. D.; Huh, J. H.; Kim, E. Y.; Park, C. C. *J. Appl. Polym. Sci.* **1998**, *69*, 1349–1355.
(55) Luo, L.; Ramirez, D.; Rood, M. J.; Grevillot, G.; Hay, K. J.; Thurston, D. L. *Carbon* **2006**, *44*, 2715–2723.
(56) Fletcher, A.; Yuzak, Y.; Thomas, K. M. *Carbon* **2006**, *44*, 989–1004.
(57) Maldonado, F. J.; Moreno-Castilla, C.; Carrasco-Marin, F.; Perez-Cadenas, A. F. *J. Hazard. Mater.* **2007**, *148*, 548–552.
(58) Tan, C.-S.; Lee, P.-L. *Environ. Sci. Technol.* **2008**, *42*, 2150–2154.
(59) Shimotori, T.; Arnold, W. A. *J. Chem. Eng. Data* **2002**, *49*, 183–190.
(60) Reza, J.; Trejo, A. *Chemosphere* **2004**, *56*, 537–547.
(61) You, Y.; Youk, J. H.; Lee, S. W.; Min, B.-M.; Lee, S. J.; Park, W. H. *Mater. Lett.* **2006**, *60*, 757–760.
(62) Kubilay, S.; Gurkan, R.; Savran, T. *Adsorption* **2007**, *13*, 41–51.